Title
Deposition Kinetics of Bioinspired Phenolic Coatings on Titanium Surfaces

Journal
Langmuir, 32(32)

ISSN
0743-7463

Authors
Geißler, Sebastian
Barrantes, Alejandro
Tengvall, Pentti
et al.

Publication Date
2016-08-16

DOI
10.1021/acs.langmuir.6b01959

Peer reviewed

HHS Public Access

Author manuscript

Langmuir. Author manuscript; available in PMC 2017 November 01.

Published in final edited form as:

Langmuir. 2016 August 16; 32(32): 8050–8060. doi:10.1021/acs.langmuir.6b01959.

Deposition Kinetics of Bioinspired Phenolic Coatings on Titanium Surfaces

Sebastian Geißler[†], **Alejandro Barrantes**[†], **Pentti Tengvall**[‡], **Phillip B. Messersmith**[§,‖,⊥], and **Hanna Tiainen**[*,†]

[†]Department of Biomaterials, Institute of Clinical Dentistry, University of Oslo, P.O. Box 1109 Blindern, 0317 Oslo, Norway

[‡]Department of Biomaterials, Institute of Clinical Sciences, Sahlgrenska Academy, University of Gothenburg, P.O. Box 412, 40530 Gothenburg, Sweden

[§]Department of Biomedical Engineering, Chemistry of Life Processes Institute, Northwestern University, Evanston, Illinois 60208, United States

[‖]Department of Bioengineering, University of California, Berkeley, Berkeley, California 94720, United States

[⊥]Department of Materials Science and Engineering, University of California, Berkeley, Berkeley, California 94720, United States

Abstract

Polyphenols can form functional coatings on a variety of different materials through auto-oxidative surface polymerization in a manner similar to polydopamine coatings. However, the mechanisms behind the coating deposition are poorly understood. We report the coating deposition kinetics of the polyphenol tannic acid (TA) and the simple phenolic compound pyrogallol (PG) on titanium surfaces. The coating deposition was followed in real time over a period of 24 h using a quartz crystal microbalance with dissipation monitoring (QCM-D). TA coatings revealed a multiphasic layer formation: the deposition of an initial rigid layer was followed by the buildup of an increasingly dissipative layer, before mass adsorption stopped after approximately 5 h of coating time. The PG deposition was biphasic, starting with the adsorption of a nonrigid viscoelastic layer which was followed by layer stiffening upon further mass adsorption. Coating evaluation by ellipsometry and AFM confirmed the deposition kinetics determined by QCM-D and revealed maximum coating thicknesses of approximately 50 and 75 nm for TA and PG, respectively. Chemical characterization of the coatings and polymerized polyphenol particles

[*]Corresponding Author: hanna.tiainen@odont.uio.no (H.T.).

The authors declare no competing financial interest.

Supporting Information

The Supporting Information is available free of charge on the ACS Publications website at DOI: 10.1021/acs.lang-muir.6b01959. Molecular structure of TA and PG; influence of different fl;ow rates on coating deposition in the QCM-D system; initial frequency shift for TA and PG; UV/vis absorbance spectra; QCM-D data for addition of fresh TA solution; QCM-D data for addition of fresh and reacted PG solution; description of QCM-D data modeling; QCM-D data for coating deposition on SiO_2; comparison of FTIRspectra of phenolic coatings and particles; QCM-D data for TA coatings using different salt concentrations; QCM-D data for PG coatings using different salt concentrations; ratio of high- and low-energy component of the O 1s peak for TA (PDF)
Video showing particle precipitation versus QCM-D results (AVI)

indicated the involvement of both physical and chemical interactions in the auto-oxidation reactions.

Graphical Abstract

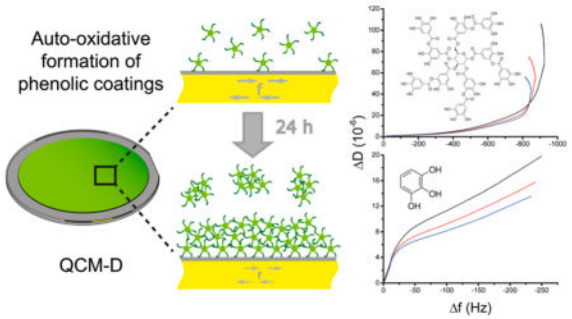

INTRODUCTION

The interaction of a material with its environment is to a great extent defined by the properties of the exposed surface. A common approach to influence the functional performance of a material is therefore to alter and improve the properties of the material surface with regard to the demands of the specific environment. The idea of using polymeric coatings to functionalize virtually any kind of material has attracted increasing attention over the past few years.[1] Among such universal coating systems, nature-derived solutions to adjust the material surface to required needs have encountered widespread interest. Probably the most renowned representative within this area is the mussel-inspired, self-polymerizing system based on polydopamine. Polydopamine coatings have been shown to be applicable to a wide range of different materials and are simple to obtain in a one-step immersion process.[2] Despite the simplicity of the coating production, the polymerization mechanisms involved in the formation of polydopamine films are complex and still a matter of investigation.[3–7] Dopamine is a small molecule consisting of a catechol group (1,2-dihydroxybenzene) with an amine group attached to it.[2] The starting point of the self-polymerization of dopamine is thought to be the auto-oxidation of the catechol group to quinone, followed by further reactions of the dopamine quinone group to 5,6-dihydroxyindole.[5–7] Several theories exist for the subsequent polymerization of these monomers, ranging from cross-linking through branching reactions, over monomer aggregation via noncovalent forces (such as hydrogen bonding, charge transfer, π-stacking), to a combination of both noncovalent and covalent interactions.[7] The catechol group of dopamine is also regarded to be responsible for the adhesive properties of polydopamine to both organic and inorganic surfaces via covalent and strong noncovalent bonding.[8] A number of binding mechanisms have been proposed for the attachment of catechols to metal oxides, including coordination bonding, bidentate chelating bonding, bridged bidentate bonding, monodentate bonding, mixed monodentate-bidentate bonding, and hydrogen bonding.[7,9] The high versatility of polydopamine coatings has led to a broad usage in different fields, e.g., in biomedical, marine antifouling, energy, or sensing applications.[7,9,10]

Inspired by such nature-derived universal coating systems, Sileika et al. have recently reported a group of molecules exhibiting similar self-polymerizing and adhesive properties based on catechol chemistry.[11] Polyphenols are products of the secondary metabolism of plants exhibiting a large number of catechol and gallol (1,2,3-trihydroxybenzene) groups.[12,13] While the precursor diversity to form polydopamine coatings is rather limited, the number of polyphenolic precursors is vast, and several have been shown to form substrate-independent coatings.[14] In addition, compared to dopamine, the coating precursors are low-cost and the coatings induce less discoloration to the substrate.[11] Of particular interest are the diverse functional properties of polyphenol-coated surfaces. Sileika et al. showed that substrates coated with the polyphenol tannic acid (TA) and the simple phenolic compound pyrogallol (PG) exhibit antioxidant properties and strong contact-based antibacterial properties while not being toxic to mammalian cells.[11] Beside these inherent properties of specific phenols and polyphenols, the adhesive nature of the coatings can be combined with further functionalization steps in order to create multifunctional surfaces. As an example, polyphenol-coated surfaces were made resistant to biofouling by functionalizing them with poly(ethylene glycol) (PEG).[11] Because of their diverse functional properties, phenolic compounds have therefore been regarded as interesting candidates for surface functionalization of medical implant materials such as titanium.[11,14–16]

While much research has been conducted to understand the mechanisms behind the coating formation of polydopamine both from a physical and chemical point of view, not much is known about these processes regarding polyphenolic surface coatings. The aim of this study was to investigate the coating deposition kinetics of self-polymerizing polyphenol systems on titanium substrates. For this purpose, we followed the coating formation of two phenolic compounds in real time over coating deposition periods up to 24 h using a quartz crystal microbalance with dissipation monitoring (QCM-D). Tannic acid (Figure S1A) was chosen due to its complex polyphenolic nature featuring the above-mentioned antioxidant and antibacterial properties. In addition, the simple phenolic compound pyrogallol (Figure S1B) was used as it represents the functional group contained in many polyphenolic compounds. QCM-D results were compared to information obtained by ellipsometry and atomic force microscopy (AFM). Moreover, the chemical properties of the polymerized coatings were characterized using X-ray photoelectron spectroscopy (XPS) and Fourier transform infrared spectroscopy (FTIR).

EXPERIMENTAL SECTION

Coating Preparation

All chemicals were purchased from Sigma-Aldrich (Oslo, Norway). Tannic acid (MW = 1701.20 g/mol) and pyrogallol (MW = 126.11 g/mol) were of ACS reagent grade. Mirror-polished, grade IV commercially pure titanium (Ti) discs and silicon wafers (Sigma-Aldrich; (100) n-type) were used as substrates for coating deposition. QCM-D studies were performed on Ti (QXS 310) and silicon dioxide (SiO_2; QXS 303) coated quartz crystals (Biolin Scientific AB, Stockholm, Sweden). All substrates were cleaned in a sonication bath, first for 15 min in 2% sodium dodecyl sulfate (SDS) followed by two times 5 min in deionized (DI) water with intermediate rinsing. The substrates were thereafter dried under

nitrogen flow, treated for 10 min in UV ozone atmosphere (PSD-UV4, Novascan Technologies, Ames, IA) and immediately used without storage.

The coating solutions were selected according to previously conducted studies.[11,17] The coating buffer for TA was made of 0.1 M bicine containing 0.6 M NaCl. For PG coatings, the buffer consisted of 0.1 M bis-tris containing 0.1 M $MgCl_2$. The pH of the buffer was adjusted to 7.8 for TA and 7.0 for PG. The phenolic compounds were dissolved in the buffers at a concentration of 1 mg/mL. The effect of salt concentration on coating formation was investigated by adjusting the NaCl concentration to either 0.3 or 0.1 M for TA solutions and the $MgCl_2$ concentration to either 0.3 or 0.2 M for PG solutions. Except for the QCM-D crystals, coatings were produced by immersing the substrates in the coating solution for up to 24 h at room temperature while shaking on a rocking platform at 30 oscillations per minute. The coated substrates were thereafter thoroughly rinsed with DI water and dried under nitrogen flow.

Evaluation of Coating Formation

The kinetics of the coating formation was investigated in real time by means of a QCM-D system (Q-Sense E4, Biolin Scientific). The freshly prepared phenolic solutions were stirred at 100 rpm with a magnetic stirrer outside the instrument while being pumped over the quartz crystals at a flow rate of 100 μL/min, unless otherwise stated. Measurements were conducted over a time period of 24 h, and temperature was kept constant at 21 °C. During coating deposition, changes in resonance frequency (Δf) and dissipation factor (ΔD) were constantly monitored. The obtained data of the third, fifth, and seventh overtones are presented in two different ways: either versus time (Δf-t and ΔD-t plots) or as ΔD versus Δf (ΔD-Δf plots). In addition, QTools software (Biolin Scientific AB) was used to obtain information about adsorbed mass and film thickness by either applying the Sauerbrey[18] or the Voigt[19] model. Sauerbrey mass and thickness for the initial stage of TA coating deposition are given as mean ± standard deviation from three different measurements. More information about the used models and modeling parameters can be found in the Supporting Information.

In addition, the absorbance of the phenolic solution used in the QCM-D experiments was measured using a Lambda 25 UV/vis spectrometer (PerkinElmer, Waltham, MA). Samples of 1 mL were collected at several different time points and filtered using a syringe filter (0.2 μm; VWR, Radnor, PA) to reduce scattering due to large polyphenol particles. UV/vis spectra of the filtered solutions were obtained at wavelength range of 230–800 nm in a quartz cuvette (104.002-QS, HellmaAnalytics, Müllheim, Germany).

Film thickness of phenolic coatings deposited on silicon wafers were measured for different coating times using an Auto-EL III null ellipsometer (Rudolph Research, Hackettstown, NJ) programmed for measurements on silicon in air. After the coating process, the wafers were rinsed with DI water and dried with nitrogen. Measurements were performed at a constant wavelength of 632.8 nm and at a constant angle of incidence of 70°. The thicknesses of the films were calculated according to the McCrackin evaluation algorithm.[20] The assumed refractive index of the phenolic films was $n_f = 1.465$. Measurements were conducted on

three spots per sample and three samples per group (n = 9). Thickness values are presented as mean ± standard deviation.

Furthermore, the obtained coatings were characterized and visualized using an atomic force microscope (MFP-3D-SA, Asylum Research, Santa Barbara, CA) in combination with OMCL-AC240TS cantilevers (Olympus Corporation, Shinjuku-ku, Japan). Partially coated samples were scanned in ac mode, and the obtained data sets were analyzed using the open source software Gwyddion. Coating thicknesses were determined by averaging the thickness of ten extracted cross-section profiles and are given as mean ± standard deviation.

Evaluation of Coating Chemistry

The chemical composition of the coated samples was analyzed by XPS and FTIR. XPS was performed on an Axis UltraDLD spectrometer (Kratos Analytical, Manchester, UK) using monochromatic Al Kα radiation ($h\nu$ = 1486.6 eV). The energy resolution was 1.1 eV for survey spectra and 0.55 eV for detail spectra, as determined by the full width at half-maximum of the Ag $3d_{5/2}$ peak of sputter-cleaned silver. Low-energy electrons were used for charge compensation, and the energy scale was corrected based on the C 1s peak of alkyl bonds, set to 284.8 eV binding energy. Detailed spectra were recorded in the energy region of O 1s and C 1s. Spectra analysis was conducted using CasaXPS (Casa Software Ltd., Teignmouth, UK), and spectra were plotted with subtracted Shirley background. FTIR spectra were obtained using a PerkinElmer Spectrum 400 FT-IR/FT-NIR spectrometer (PerkinElmer, Waltham, MA). Coated substrates were measured with a diffuse reflectance accessory in the mid-infrared range between 4000 and 450 cm^{-1}. The background spectrum was collected from an unmodified sample. For powder and particle samples, the attenuated total reflectance (ATR) accessory was used in the range between 4000 and 650 cm^{-1}. Per sample, 16 scans with a resolution of 4 cm^{-1} were conducted. Spectra obtained by both XPS and FTIR were compared to the spectra of precursor powders of TA and PG. Furthermore, 10 mL of each reacted coating solution was filtered (0.22 μm GSWP, Millipore, Billerica, MA) and rinsed with 5 × 100 mL water using a Büchner funnel. The obtained particles were air-dried overnight before characterization.

RESULTS AND DISCUSSION

Use of the QCM-D System To Determine Reaction Kinetics of Phenolic Coatings

TA and PG films were produced on titanium surfaces by immersing the substrates in the coating solutions while being agitated on a rocking platform as reported by Sileika et al.[11] To examine the deposition kinetics of the phenolic films, these coating conditions had to be transferred into the QCM-D setup. Unlike in previous studies, where the deposition of polydopamine was investigated by introducing single injections of dopamine solution into the QCM-D system,[21,22] we applied a continuous flow system to better simulate the real coating conditions rather than having a layer-by-layer deposition of several thin films. The agitation of the rocking platform was mimicked by stirring the phenolic solutions outside the QCM-D system, ensuring sufficient supply of oxygen that is required for the oxidation reaction.[21] Simultaneously to this stirring, the phenolic solutions were constantly pumped into the QCM-D system and over the quartz crystals, where the interactions with the

substrate surface were monitored. The flow rate used for pumping the phenolic solutions over the quartz crystals had an influence on the coating formation and was optimized in the used setup (see Supporting Information, Figure S2). Under real coating conditions, the reaction processes in the solution and the adsorption process to the substrate occur simultaneously. The separation of these two processes in the QCM-D setup might introduce systematic errors which should be considered when interpreting the obtained results.

Deposition Kinetics of Tannic Acid

The deposition kinetics of TA on titanium-coated quartz crystals was followed by QCM-D over a coating time of 24 h. An initial negative frequency shift was observed immediately after the coating solution came in contact with the crystal surface (Figure S3A). This frequency shift of $\Delta f \sim -15$ Hz occurred within the first 30 s and is therefore likely to correspond to the first layer of TA molecules attaching to the titanium oxide surface, possibly through coordination via TiO(OH)TA hydroxo complexes.[23] A similar behavior was observed by other groups when studying the adsorption of dopamine on SiO_2-coated quartz crystals[22] and TA on gold- and SiO_2-coated quartz crystals.[24] While in our experiments, the frequency continued to decrease after this initial fast frequency change, both of the above-mentioned studies reported a leveling of the frequency. These differences in the initial coating behavior might be explained by differences in the coating systems. Bernsmann et al. injected only single volumes of fresh dopamine solution, and these noncontinuous flow conditions could have caused the leveling of the frequency after the initial dopamine adsorption.[22] The deposition of TA in the work by Ball and Meyer was done under continuous flow, however, at a pH of 5.0 where TA does not oxidize.[24] The interactions between TA molecules in solution and the reactions of the molecules with the substrate are therefore regarded to be different compared to the present study, forming only an adsorbed monolayer on the quartz crystal. The constant supply of new reaction partners in our study led to a further TA layer buildup which could be divided into three distinct growth phases as shown in Figure 1.

The first phase up to 2 h of coating time was characterized by a rapid decrease in frequency to $\Delta f \sim$ -400 Hz and a small change in dissipation of $\Delta D < 5 \times 10^{-6}$ (Figure 1A). Plotting the dissipation change versus the frequency change resulted in a virtually horizontal curve, highlighted with an arrow pointing toward negative frequency values in Figure 1B. This phase represents the buildup of a very compact and rigid coating.[25,26] In the second phase up to approximately 5 h, a further decrease in frequency was accompanied by a strong increase in dissipation. The higher slope in the ΔD-Δf plot in this phase indicates that while TA kept adsorbing to the surface, the layer became softer compared to the initial layer.[26] In the third phase, Δf leveled out at approximately -900 Hz, while the dissipation kept increasing up to 24 h of coating time at a slower rate than in the second phase. In the ΔD-Δf plot, this phase was characterized by a vertical curve toward positive dissipation values revealing the stop in mass adsorption, while the layer still underwent structural changes.[26]

The similarity between the phenolic systems and the dopamine system suggests that similar mechanisms are involved in the coating formation and self-polymerization process. Since the presence of oxygen is a necessary requirement for successful coating formation, it is likely

that oxidation processes play a key role in the coating buildup.[11] The formation of reactive quinones which further aggregate to higher molecular weight species are believed to be responsible for the self-polymerization.[11,14] This theory was supported by two observations in the present study: First, a color change of the TA solutions from almost colorless to dark green was seen with progressing coating time. This color change has previously been found to be largely suppressed in anaerobic conditions.[11] Second, large agglomerates formed in the coating solution and precipitated to the bottom of the reaction beaker. Interestingly, this precipitation occurred after approximately 5 h, which corresponds to the time point at which the frequency in the QCM-D reached a constant level (see video in Supporting Information). Furthermore, the particle precipitation coincided with a clear change in UV/vis absorbance spectrum from the gradual shift of the absorbance peak initially having a maximum at approximately 360 nm to higher wavelengths to the emergence of more pronounced features in the visible range of the spectrum (Figure S4A,B). Therefore, we assume that the size of the particles and their reduced interaction capability with the existing coating limited further growth of the TA layer due to depletion of reactive precursor molecules from the solution. In order to test this assumption, TA deposition was stopped after 4 h, the QCM-D crystals were rinsed with buffer, and freshly prepared TA solution was pumped over the coated crystals. The frequency and dissipation changes continued similar to the preceding part of coating deposition, and no leveling of the frequency was observed (Figure S5). Thus, the supply of fresh TA solution could prolong the coating buildup, indicating that the depletion of reactant from the coating solution was the limiting factor for further coating formation. This supports the assumed role of particle size and reactivity in the coating formation process: in the beginning of the coating deposition, TA molecules start to react with the substrate as well as with other TA molecules in solution. The resulting complexes attaching to the surface are still relatively small and form a rigid film on the substrate (phase 1 in Figure 1). As the coating deposition proceeds, the particles attaching to the surface get larger and contribute therefore more and more to the change in coating structure (increasing dissipation factor in phase 2). Water coupling through hydration, viscous drag, or entrapment in cavities between the TA particles is also likely to occur in this phase.[27] Once a critical size is reached, the particles precipitate, stop attaching to the existing coating, and no further mass adsorption is observed (phase 3). Hence, the presence of small and reactive TA species seems to be a requirement for the buildup of the coating. Our findings are consistent with those obtained by Bernsmann et al. for the deposition of dopamine on silicon oxide.[22] They observed that advanced polymerization and aggregation of dopamine in solution did not result in further coating formation, highlighting the critical role of unreacted monomers or small oligomers in the coating process.[22] The reason why the dissipation still increased in the last phase of coating deposition remains unclear. However, the largest increase was observed for the third overtone which is sensing furthest away from the crystal surface compared to the other two overtones.[26,28] The detected dissipation change could therefore be a result of large TA particles flowing past the quartz crystal surface without attaching to the existing coating. Another possible explanation could be the occurrence of remodeling processes within the outermost layer of the TA coating, such as dynamic reconfigurations, detachment and reattachment of TA particles, water exchange, or combinations of the aforementioned.[29]

Deposition Kinetics of Pyrogallol

In contrast to TA coatings, only two growth phases could be distinguished for PG coating deposition (Figure 2). Moreover, the initial frequency decrease was less pronounced for PG coatings with $\Delta f \sim$ 1–2 Hz within the first minutes after injection (Figure S3B). Following this, a moderate decrease in frequency combined with a fast increase in dissipation was observed during the first 2–3 h of coating deposition (phase 1 in Figure 2A). This phase was characterized by a high slope in the ΔD-Δf plot toward positive dissipation and negative frequency values, corresponding to the buildup of a nonrigid viscoelastic layer.[26] After this, the deposition kinetics changed to a slower increase in dissipation while the frequency shift became more rapid. Both changes in frequency and dissipation factor were nearly constant reaching values of approximately −250 Hz and 20×10^{-6}, respectively, in the third overtone after 24 h. This kinetics change is represented by a decrease in the slope of the ΔD-Δf plot, suggesting that the layer became more compact and rigid upon further mass adsorption.

During the coating process, a distinct color change of the PG coating solutions to orange and dark brown was observed (see video in Supporting Information). This supports the previously assumed involvement of quinone intermediates in the polymerization reaction of the phenolic compounds. According to Haslam, polyphenols which are composed of one or more *ortho*-di- or trihydroxy phenyl groups can undergo auto-oxidation at pH values around 7.0 or higher.[30] The oxidative formation of *ortho*-quinones results in a characteristic orange or red color,[30] being consistent with the observations made in the present study. We assume that the formation of reactive quinones, which subsequently interact with each other in the coating solution, is the predominant reaction in the first phase of PG coating formation. In this stage, only small amounts of the reaction products attached to the quartz crystal as seen by the low frequency shift in the QCM-D data (Figure 2). Furthermore, the relatively high dissipation per coupled unit mass might be a sign for a nonuniform or only loosely interconnected coating. With progressing coating time, more complex polyphenolic compounds formed in the coating solution and the reduced solubility of these complexes resulted in higher interaction with the substrate surface. The larger mass adsorption in this second phase might have led to a stiffening of the layer as indicated by the change in dissipation compared to the first phase.

In contrast to TA coatings, the coating deposition did not level off and continued up to the monitored coating time of 24 h. This might be due to the following reasons: PG is a much smaller molecule compared to TA (126.11 g/mol vs 1701.20 g/ mol). Since the formation of particles was not as distinct as for TA, we think that PG particles do not grow as large as TA particles, and those particles are still reactive enough to interact with the existing coating. In addition, at the given mass concentration of 1 mg/mL, the molar concentration of PG is higher compared to TA solutions. Moreover, the mechanisms of complexation might be different for TA and PG. In enzyme-catalyzed reactions, it has been shown that simpler phenolic compounds are first oxidized to quinones, which then are involved in a coupled redox system to oxidize more complex polyphenols while being reduced back to the free phenolic state.[30] Hence, when more complex polyphenolic compounds are formed during PG auto-oxidation, quinones generated from PG could also be reduced back and therefore would stay available for further reactions. In contrast, such simple phenolic compounds are

not present in TA solution. Once larger TA complexes are formed, there might be no more or not enough reactive partners present to continue the reaction.

Difference in the reaction mechanism was in fact observed in the UV/vis spectra of PG and TA. Whereas a very gradual peak shift was seen for TA during the first 30 min reaction time, a rapid appearance of a peak at 325 nm, which has been associated with the dissociation of the phenolic OH groups resulting in resonant structures in polyphenolic molecules,[31,32] was observed for PG solutions (Figure S4). Over time, the PG spectrum started gradually resembling the spectrum observed for TA, indicating that more complex polyphenolic molecules were formed during the early time points (until 1 h) of the polymerization reaction. Furthermore, the apparent similarity of the absorbance spectrum suggests that the auto-oxidative polymerization following the initial formation of more complex polyphenolic compounds occurs by similar mechanism for both TA and PG molecules.

The presence of two different reaction phases in PG coating deposition was further verified by exchanging the coating solution after 2 h of coating deposition to either fresh PG solution or PG solution that had already been reacting for more than 24 h (Figure S6). While the addition of fresh PG solution did not change the coating kinetics and only slow frequency shifts similar to the first phase in Figure 2 were observed, a significant kinetics change was seen after the addition of reacted PG solution. The reacted solution led to a more rapid and stable frequency change which corresponded to the second phase in Figure 2. These observations confirmed that an initial polymerization reaction of PG monomers or small PG complexes in solution is needed before a constant coating buildup takes place.

Correlation of QCM-D Results with Real Coating Conditions

In order to verify that the determined deposition kinetics in fact apply to the coating formation under real coating conditions, the QCM-D results were compared to information obtained by ellipsometry and AFM. For this purpose, modeling of the QCM-D data was performed to get the thicknesses of the phenolic coatings on the quartz crystals (see Supporting Information for modeling details and parameters). The Sauerbrey thickness of the TA layer deposited during the first hour is displayed in Figure 3A. An initial fast increase in coating thickness to approximately 2–3 nm was seen which correlates to the initial negative frequency shift (Figure S3A). Assuming the molecular dimensions of TA to be 1.85 × 1.65 × 1.01 nm^3 and the hydrodynamic diameter to be less than 1.63 nm at the used pH,[33] this would mean that the initial layer corresponded to more than a monolayer of TA molecules adsorbed to the surface. Therefore, it is likely that TA molecules had already formed small complexes in solution before attaching to the substrate. The coating thickness increased thereafter to 28.15 ± 2.64 nm after 60 min of coating time, corresponding to a mass of 3.38 ± 0.32 $\mu g/cm^2$. For longer coating times, the Sauerbrey assumption of a rigid film adsorbed to the surface could no longer be regarded as valid model due to the large increase in dissipation (phases 2 and 3 in Figure 1).

Thus, we tried to apply the Voigt model for viscoelastic films to determine the film thickness,[19,34] but it was impossible to get a good agreement between the modeled and the measured data. The reason for this could be the complexity of the TA films after long coating times. We assume that the continuous TA particle growth in the coating solution

leads to a gradual change in surface structure when particles of different size attach to the already existing coating, making the application of the model difficult. On the other hand, a good fit was obtained when the Voigt model was applied to the data measured for PG coatings (Figure 3B). The thickness increased constantly up to approximately 49 nm after 24 h.

The use of ellipsometry on coated titanium discs was unsuccessful due to variations in substrate optical constants and high variations in modeling outcome, especially for thin coatings. Since the deposition kinetics of the phenolic coatings on SiO_2 was comparable to that on TiO_2 surfaces (Figure S7), coating thicknesses were measured on silicon wafers using a system programmed for measurements on Si/SiO_2 in air. The coating thicknesses determined by ellipsometry exhibited similar growth trends to the ones observed in the QCM-D measurements. TA coatings showed a rapid increase in thickness up to 4 h, after which a plateau at approximately 50 nm was reached (Figure 4A). After 60 min coating time, the measured thickness was approximately half the thickness calculated using the Sauerbrey relation (Figure 4B). Lower thickness values measured by ellipsometry were expected as QCM-D quantifies not only the adsorbed mass but also its associated water.[35] These findings are consistent with those by Bernsmann et al. for polydopamine coatings, indicating a deswelling of the hydrated TA coating during drying with nitrogen.[22] After 24 h, no coating could be detected on any of the measured SiO_2 samples. We suppose that the low surface roughness of the silicon wafers had an influence on the coating stability for such long coating times. The anchorage of the coating on the smooth surface was probably not strong enough to prevent detachment of the highly dissipative and hydrated film while rinsing after the coating. The average coating thickness of 20 h coatings determined by AFM was 53.0 ± 3.7 nm and confirmed the thickness measured by ellipsometry (Figure 5A). Moreover, AFM scans showed a uniform TA coating exhibiting some large agglomerates which probably originated from adsorption of large TA particles from the reacted TA solution.

Ellipsometry measurements of PG coatings revealed almost no thickness increase within the first 60 min (Figure 4C). This finding is consistent with the observed low initial frequency shifts in the QCM-D experiments (Figure 2A). For longer coating times, a constant increase in thickness was observed up to approximately 75 nm after 24 h (Figure 4C). AFM measurements of 24 h coatings revealed an average thickness of 49.9 ± 9.7 nm (Figure 5B), which matched the thickness calculated from the QCM-D data. PG coatings did not cover the substrate surface as uniformly as TA coatings, and several spots with very thin or no coatings were seen alongside very large agglomerates. This inhomogeneity might explain the higher thickness values determined by ellipsometry, since ellipsometry averages over a large surface area (~0.6 mm^2). Furthermore, the fact that the AFM thickness was equal to the QCM-D thickness indicates that PG coatings were less hydrated compared to TA coatings, and thus less deswelling of the layer occurred during the drying step.

Chemical Characterization of Phenolic Coatings

FTIR scans of TA and PG coated titanium discs revealed changes in the infrared spectra compared to the corresponding precursor powder. However, the band intensities in these

spectra obtained with the diffuse reflectance accessory were very weak, in particular for PG coatings (Figure S8). For this reason, FTIR scans of the polymerized particles formed in the coating solutions were conducted, assuming that the particles were of the same nature as the phenolic coatings on titanium substrates. As shown in Figure S8, the infrared spectra of the particles exhibited the same characteristics as those of the coatings, yet showing clearer bands and therefore facilitating the analysis. The infrared spectra of the particles were thereafter compared to those of the precursor powders (Figure 6).

Both TA powder and particles showed a strong and broad band at 3308 and 3311 cm^{-1}, respectively. These bands were assigned to O-H stretching vibrations of the phenolic hydroxyl groups, while the broadness of the bands is a sign for intramolecular hydrogen bonds.[36–38] The fact that the band got narrower for the reacted TA particles suggests a partial breakup of the intramolecular hydrogen bonds due to interaction with other TA molecules.[37] The band at 1700 cm^{-1} in the TA powder spectrum was assigned to C O stretching vibrations of the carboxylic acid groups in TA.[36,39] The shift of this band to 1669 cm^{-1} in the particle spectrum was attributed to hydrogen bonding to the C═O group.[36] The infrared spectrum obtained for the PG precursor powder corresponded well with spectra previously reported.[40] The broad band composed of multiple peaks in the area around 3228 cm^{-1} was again assigned to phenolic hydroxyl stretching vibrations.[36–38] In the spectrum of PG particles, no clear peaks were distinguishable in this region, and the overall band appeared broader. Furthermore, a distinct change of the band at 1189 cm^{-1} was seen which was assigned to O-H in-plane bending.[40] These changes give an indication that hydroxyl groups are involved in the polymerization reaction of PG. For both TA and PG, most noticeable changes occurred in the region around 1300 cm^{-1} (highlighted in Figure 6). This region can be assigned to a combination of O-H deformation vibrations and C-O stretching vibrations of phenols.[36] Generally, the clear differences in the infrared spectra of the precursors and the reacted particles suggest that not only physical but also chemical interactions are involved in the self-polymerization process.

XPS was used to assess the elemental composition of the precursor powders, phenolic coatings on titanium discs, and polymerized particles (Table 1). Measurements of PG precursor powder were not successful due to the high reactivity and instant oxidation of the powder, resulting in high discrepancy between measured and theoretical C/O ratios. The C/O ratios for the other groups were in comparable ranges as previously described.[11] For both the coatings and the polymerized particles, Na and Mg were detected for TA and PG, respectively. This finding was not unexpected since the coating solutions contained either NaCl or $MgCl_2$. However, only small amounts or no Cl were found in both reaction products. The presence of Na and Mg can thus not be explained merely by the presence of salt. Since metal ions such as Na and Mg can play a role in the formation of polymer networks,[41] we assume that the ions are part of the coatings and particles, probably acting as binding partners through coordination bonding similar to the reported interaction of transition metals with polyphenols.[31,42–45] This assumption was tested by changing the salt concentration in the TA coating solutions. The start of frequency and dissipation changes was noticeably delayed with reduced salt concentrations (Figure S9A,B). Also, the color change occurred much slower and did not result in as intense green color as observed for the high salt concentration. Furthermore, reduced salt concentrations did not lead to formation

of a uniform TA coating after the initial adsorbed layer, which caused the previously observed frequency shift of approximately 15 Hz. After this, no change in frequency was observed until particle precipitation occurred, resulting in rapid change in both frequency and dissipation simultaneously without further coating formation (Figure S9C). Conversely, increase in salt concentration appeared to result in delayed coating formation for PG, although the change in formation kinetics was not as pronounced as seen for TA (Figure S10). Thus, the presence and concentration of metal ions in the coating solutions seemed to have a significant influence on the self-polymerization and coating formation process.

The peaks in the C 1s and O 1s detail spectra of the TA precursor powder were assigned according to the molecular structure of TA (Figure 7A,B; see Figure S1 for molecular structure of TA).[46] The C 1s peak exhibited components characteristic of an organic compound containing aromatic rings and showed no obvious changes for the TA coatings and the polymerized TA particles (Figure 7B,D). Deconvolution of the O 1s peak was difficult due to multiple overlapping component contributions (Figure 7A). Moreover, the presence of hydrogen bonds, which was detected in the FTIR analysis, can lead to peak shifts in the XPS spectra and therefore complicates the exact peak assignment.[47] For the ease of analysis, the O 1s peak was divided into a high- and low-energy component centered at ~533.4 and ~531.8 eV, respectively. While the elemental distribution of oxygen remained unchanged for TA coatings and particles (~35 at. %; Table 1), a clear intensity reduction of the high energy component and an intensity increase of the low-energy component of the O 1s peak was observed (Figure 7C and Table S2). Such an increase of the low-energy contribution to the O 1s peak has previously been seen for polyphenol-metal ion complexation.[31,44,45] The intensity decrease of the high-energy component, which contains the contribution of the C-OH groups, strengthens the assumed role of the hydroxyl groups in the polymerization reaction, as already indicated by the FTIR results.

The detailed spectra of PG coatings and polymerized PG particles could not be compared to the precursor powder. However, the O 1s peak exhibited similar energy components as seen in the TA spectra, and the low-energy component had the same intensity as the high-energy component (Figure 7E). Beside the above-mentioned potential contribution of metal-polyphenol complexes to this low-energy component, also the O═C component can be found in this energy region.[46] Since the PG molecule does not contain carbon-oxygen double bonds (Figure S1B), this could be an indication of the presence of quinone groups.

CONCLUSIONS

QCM-D was applied to continuously monitor the auto-oxidative coating deposition of the two phenolic compounds tannic acid (TA) and pyrogallol (PG) on titanium surfaces over deposition periods of 24 h. TA coatings revealed multiple growth phases: after the buildup of a very compact and rigid coating up to ~2 h, the adsorption of an increasingly dissipative layer was observed up to ~5 h. The discontinuation in coating deposition after ~5 h correlated with the precipitation of large particles in the coating solutions, likely depleting the solution of TA precursors. PG coating deposition occurred in two growth phases: an initial deposition of a nonrigid viscoelastic layer up to 2–3 h was followed by layer stiffening with continuing mass adsorption up to 24 h. The growth in coating thickness

determined by ellipsometry was consistent with the coating kinetics determined by QCM-D. While TA coating thickness reached a plateau at approximately 50 nm, PG coatings continuously increased in thickness up to approximately 75 nm after 24 h. Chemical characterization of the coatings and reacted polyphenol particles indicated that both physical and chemical interactions were involved in the auto-oxidation process. Metal ions (Na and Mg) were present in the deposited TA and PG coatings, and the concentration of these ions in the coating buffer was found to influence the deposition kinetics, indicating that metal ion coordination may be involved in the auto-oxidation process of the phenolic molecules.

Supplementary Material

Refer to Web version on PubMed Central for supplementary material.

Acknowledgments

The authors thank Martin F. Sunding and Jonas Wengenroth for their technical assistance with XPS and AFM characterization. This work was supported by the Research Council of Norway (Grant 230258). The authors acknowledge the Scandinavian Society for Biomaterials (ScSB) and the Research Council of Norway for providing travel grants for Sebastian Geißler to perform experiments at University of Gothenburg and Northwestern University, respectively. This research was partially supported by National Institutes of Health Grant R37 DE014193.

References

1. Wei Q, Haag R. Universal polymer coatings and their representative biomedical applications. Mater Horiz. 2015; 2:567–577.
2. Lee H, Dellatore SM, Miller WM, Messersmith PB. Mussel-inspired surface chemistry for multifunctional coatings. Science. 2007; 318:426–30. [PubMed: 17947576]
3. d'Ischia M, Napolitano A, Ball V, Chen CT, Buehler MJ. Polydopamine and eumelanin: from structure-property relationships to a unified tailoring strategy. Acc Chem Res. 2014; 47:3541–3550. [PubMed: 25340503]
4. Yang J, Cohen Stuart MA, Kamperman M. Jack of all trades: versatile catechol crosslinking mechanisms. Chem Soc Rev. 2014; 43:8271–8298. [PubMed: 25231624]
5. Hong S, Na YS, Choi S, Song IT, Kim WY, Lee H. Non-covalent self-assembly and covalent polymerization co-contribute to polydopamine formation. Adv Funct Mater. 2012; 22:4711–4717.
6. Della Vecchia NF, Avolio R, Alfè M, Errico ME, Napolitano A, d'Ischia M. Building-block diversity in polydopamine underpins a multifunctional eumelanin-type platform tunable through a quinone control point. Adv Funct Mater. 2013; 23:1331–1340.
7. Liu Y, Ai K, Lu L. Polydopamine and its derivative materials: synthesis and promising applications in energy, environmental, and biomedical fields. Chem Rev. 2014; 114:5057–5115. [PubMed: 24517847]
8. Lee H, Scherer NF, Messersmith PB. Single-molecule mechanics of mussel adhesion. Proc Natl Acad Sci U S A. 2006; 103:12999–13003. [PubMed: 16920796]
9. Ye Q, Zhou F, Liu W. Bioinspired catecholic chemistry for surface modification. Chem Soc Rev. 2011; 40:4244–58. [PubMed: 21603689]
10. Sedó J, Saiz-Poseu J, Busquè F, Ruiz-Molina D. Catechol-based biomimetic functional materials. Adv Mater. 2013; 25:653–701. [PubMed: 23180685]
11. Sileika TS, Barrett DG, Zhang R, Lau KHA, Messersmith PB. Colorless multifunctional coatings inspired by polyphenols found in tea, chocolate, and wine. Angew Chem, Int Ed. 2013; 52:10766–10770.
12. Quideau S, Deffieux D, Douat-Casassus C, Pouységu L. Plant polyphenols: chemical properties, biological activities, and synthesis. Angew Chem, Int Ed. 2011; 50:586–621.

13. Bravo L. Polyphenols: Chemistry, dietary sources, metabolism, and nutritional significance. Nutr Rev. 1998; 56:317–333. [PubMed: 9838798]
14. Barrett DG, Sileika TS, Messersmith PB. Molecular diversity in phenolic and polyphenolic precursors of tannin-inspired nanocoatings. Chem Commun. 2014; 50:7265–7268.
15. Cordoba A, Satue M, Gomez-Florit M, Hierro-Oliva M, Petzold C, Lyngstadaas SP, Gonzalez-Martin ML, Monjo M, Ramis JM. Flavonoid-modified surfaces: multifunctional bioactive biomaterials with osteopromotive, anti-inflammatory, and anti-fibrotic potential. Adv Healthcare Mater. 2015; 4:540–549.
16. Gomez-Florit M, Pacha-Olivenza MA, Fernández-Calderón MC, Córdoba A, González-Martín ML, Monjo M, Ramis JM. Quercitrin-nanocoated titanium surfaces favour gingival cells against oral bacteria. Sci Rep. 2016; 6:22444. [PubMed: 26925553]
17. Messersmith, PB., Sileika, TS., Zhang, R., Barrett, DG. Phenolic coatings and methods of making and using same. US Patent Application. 20140228306. Feb 24. 2014
18. Sauerbrey G. The use of quartz oscillators for weighing thin layers and for microweighing. Eur Phys J A. 1959; 155:206–222.
19. Voinova MV, Rodahl M, Jonson M, Kasemo B. Viscoelastic acoustic response of layered polymer films at fluid-solid interfaces: continuum mechanics approach. Phys Scr. 1999; 59:391–396.
20. McCrackin FL. A Fortran program for analysis of ellipsometer measurements. NBS Technical Note. 1969; 479
21. Bernsmann F, Frisch B, Ringwald C, Ball V. Protein adsorption on dopamine-melanin films: role of electrostatic interactions inferred from zeta-potential measurements versus chemisorption. J Colloid Interface Sci. 2010; 344:54–60. [PubMed: 20092826]
22. Bernsmann F, Ponche A, Ringwald C, Hemmerle J, Raya J, Bechinger B, Voegel JC, Schaaf P, Ball V. Characterization of dopamine-melanin growth on silicon oxide. J Phys Chem C. 2009; 113:8234–8242.
23. Surleva A, Atanasova P, Kolusheva T, LC. Study of the complex equilibrium between titanium (IV) and tannic acid. J Chem Technol Metall. 2014; 49:594–600.
24. Ball V, Meyer F. Deposition kinetics and electrochemical properties of tannic acid on gold and silica. Colloids Surf, A. 2016; 491:12–17.
25. Rodahl M, Höök F, Fredriksson C, Keller CA, Krozer A, Brzezinski P, Voinova M, Kasemo B. Simultaneous frequency and dissipation factor QCM measurements of biomolecular adsorption and cell adhesion. Faraday Discuss. 1997; 107:229–246.
26. McCubbin GA, Praporski S, Piantavigna S, Knappe D, Hoffmann R, Bowie JH, Separovic F, Martin LL. QCM-D fingerprinting of membrane-active peptides. Eur Biophys J. 2011; 40:437–446. [PubMed: 21161523]
27. Höök F, Kasemo B, Nylander T, Fant C, Sott K, Elwing H. Variations in coupled water, viscoelastic properties, and film thickness of a Mefp-1 protein film during adsorption and cross-linking: a quartz crystal microbalance with dissipation monitoring, ellipsometry, and surface plasmon resonance study. Anal Chem. 2001; 73:5796–804. [PubMed: 11791547]
28. Mechler A, Praporski S, Atmuri K, Boland M, Separovic F, Martin LL. Specific and selective peptide-membrane interactions revealed using quartz crystal microbalance. Biophys J. 2007; 93:3907–3916. [PubMed: 17704161]
29. Hovgaard MB, Dong M, Otzen DE, Besenbacher F. Quartz crystal microbalance studies of multilayer glucagon fibrillation at the solid-liquid interface. Biophys J. 2007; 93:2162–2169. [PubMed: 17513349]
30. Haslam, E. Practical Polyphenolics - From Structure to Molecular Recognition and Physiological Action. Cambridge University Press; Cambridge: 1998.
31. Rahim MA, Ejima H, Cho KL, Kempe K, Müllner M, Best JP, Caruso F. Coordination-driven multistep assembly of metal-polyphenol films and capsules. Chem Mater. 2014; 26:1645–1653.
32. Tóth IY, Szekeres M, Turcu R, Sáringer S, Illés E, Nesztor D, Tombácz E. Mechanism of in situ surface polymerization of gallic acid in an environmental-inspired preparation of carboxylated core-shell magnetite nanoparticles. Langmuir. 2014; 30:15451–15461. [PubMed: 25517214]

33. Oćwieja M, Adamczyk Z, Morga M. Adsorption of tannic acid on polyelectrolyte monolayers determined in situ by streaming potential measurements. J Colloid Interface Sci. 2015; 438:249–258. [PubMed: 25454449]
34. Macakova L, Blomberg E, Claesson PM. Effect of adsorbed layer surface roughness on the QCM-D response: focus on trapped water. Langmuir. 2007; 23:12436–12444. [PubMed: 17944494]
35. Höök F, Vöroös J, Rodahl M, Kurrat R, Boöni P, Ramsden JJ, Textor M, Spencer ND, Tengvall P, Gold J, Kasemo B. A comparative study of protein adsorption on titanium oxide surfaces using in situ ellipsometry, optical waveguide lightmode spectroscopy, and quartz crystal microbalance/dissipation. Colloids Surf, B. 2002; 24:155–170.
36. Socrates, G. Infrared and Raman Characteristic Group Frequencies. John Wiley & Sons, LTD; Chichester: 2001.
37. Huang X, Wu H, Liao X, Shi B. One-step, size-controlled synthesis of gold nanoparticles at room temperature using plant tannin. Green Chem. 2010; 12:395–399.
38. Bulut E, Özacar M. Rapid, facile synthesis of silver nanostructure using hydrolyzable tannin. Ind Eng Chem Res. 2009; 48:5686–5690.
39. Stuart, B. Biological Applications of Infrared Spectroscopy. John Wiley & Sons; Chinchester: 1997.
40. Mohammed-Ziegler I, Billes F. Vibrational spectroscopic calculations on pyrogallol and gallic acid. J Mol Struct: THEOCHEM. 2002; 618:259–265.
41. Fromm KM. Coordination polymer networks with s-block metal ions. Coord Chem Rev. 2008; 252:856–885.
42. Ejima H, Richardson JJ, Liang K, Best JP, van Koeverden MP, Such GK, Cui JW, Caruso F. One-step assembly of coordination complexes for versatile film and particle engineering. Science. 2013; 341:154–157. [PubMed: 23846899]
43. Ringwald C, Ball V. Layer-by-layer deposition of tannic acid and Fe(3)(+) cations is of electrostatic nature but almost ionic strength independent at pH 5. J Colloid Interface Sci. 2015; 450:119–26. [PubMed: 25805445]
44. Mao H, Liao Y, Ma J, Zhao SL, Huo FW. Water-soluble metal nanoparticles stabilized by plant polyphenols for improving the catalytic properties in oxidation of alcohols. Nanoscale. 2016; 8:1049–1054. [PubMed: 26662453]
45. Mao H, Yu H, Chen J, Liao X. Biphasic catalysis using amphiphilic polyphenols-chelated noble metals as highly active and selective catalysts. Sci Rep. 2013; 3:2226. [PubMed: 23863916]
46. Beamson, G., Briggs, D. High Resolution XPS of Organic Polymers: the Scienta ESCA300 Database. Wiley; New York: 1992.
47. Patrick CE, Giustino F. O 1s core-level shifts at the anatase TiO_2(101)/N3 photovoltaic interface: Signature of H-bonded supra- molecular assembly. Phys Rev B: Condens Matter Mater Phys. 2011; 84:085330.

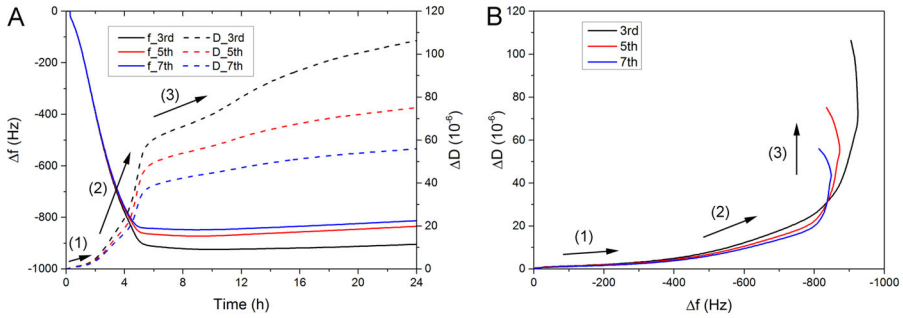

Figure 1.

(A) Δ*f*-*t* and Δ*D*-*t* plots and (B) Δ*D*-Δ*f* plot showing the third, fifth, and seventh overtone for tannic acid (TA) deposition on Ti surfaces as recorded by QCM-D over a time period of 24 h. Three distinct coating phases were observed and are highlighted with numbered arrows.

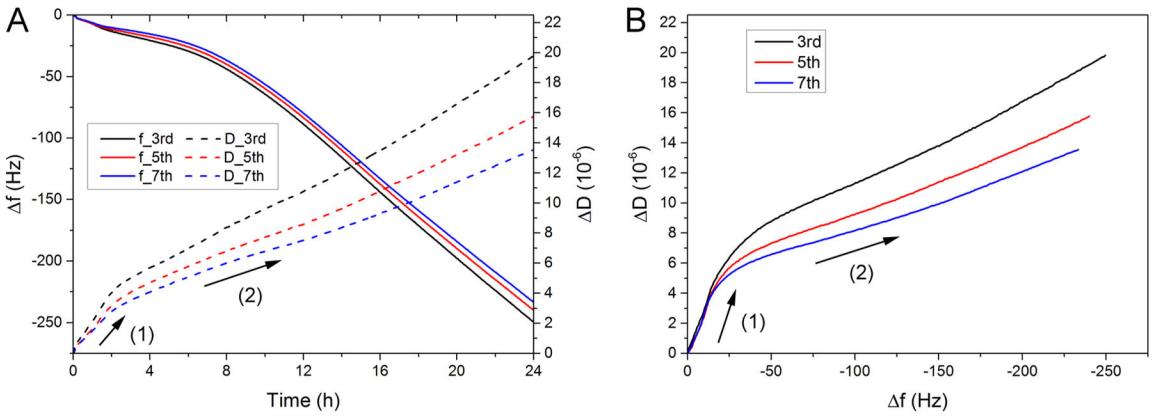

Figure 2.

(A) Δ*f*-*t* and Δ*D*-*t* plots and (B) Δ*D*-Δ*f* plot showing the third, fifth, and seventh overtone for pyrogallol (PG) deposition on Ti surfaces as recorded by QCM-D over a time period of 24 h. Two different coating phases were observed and are highlighted with numbered arrows.

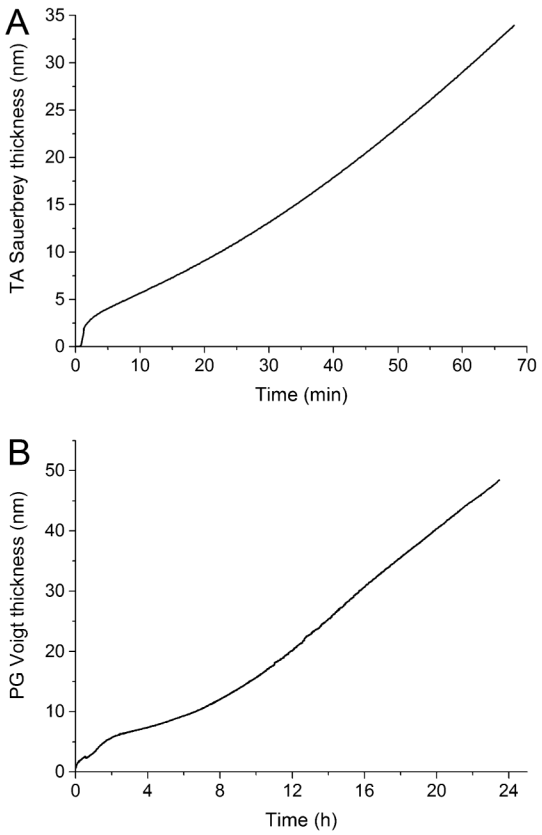

Figure 3.

(A) Tannic acid (TA) coating thickness for the initial coating stage calculated using the Sauerbrey relation. (B) Pyrogallol (PG) coating thickness for 24 h of coating time calculated using the Voigt model for viscoelastic films.

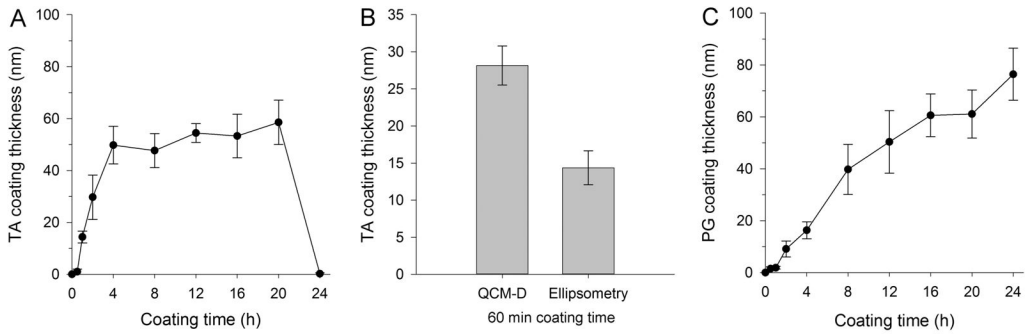

Figure 4.

(A) Thickness of tannic acid (TA) coatings measured by ellipsometry up to 24 h of coating time. The thickness reached a constant level at approximately 50 nm after 4 h. No coatings could be detected on TA samples coated for 24 h. (B) Comparison of TA coating thickness obtained by QCM-D and ellipsometry for coating times of 60 min. The coating thickness determined by ellipsometry was approximately half the thickness calculated from the QCM-D data. (C) Thickness of pyrogallol (PG) coatings measured by ellipsometry. The coatings exhibited a continuous increase in thickness up to 24 h of coating time.

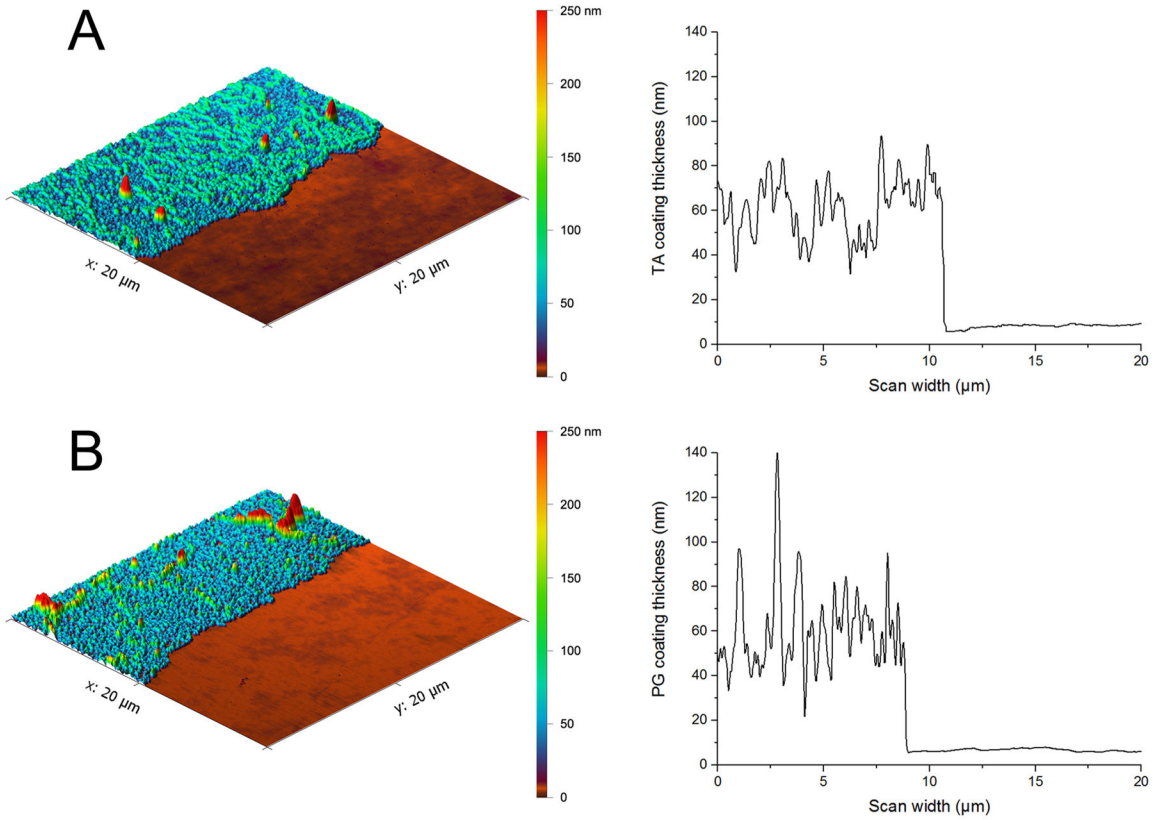

Figure 5.

AFM images of silicon wafers partially coated with (A) tannic acid (TA) for 20 h and (B) pyrogallol (PG) for 24 h. On the right-hand side, cross-section profiles of the respective scans are displayed. The average coating thickness calculated from 10 extracted profile lines was 53 ± 4 nm for TA and 50 ± 10 nm for PG.

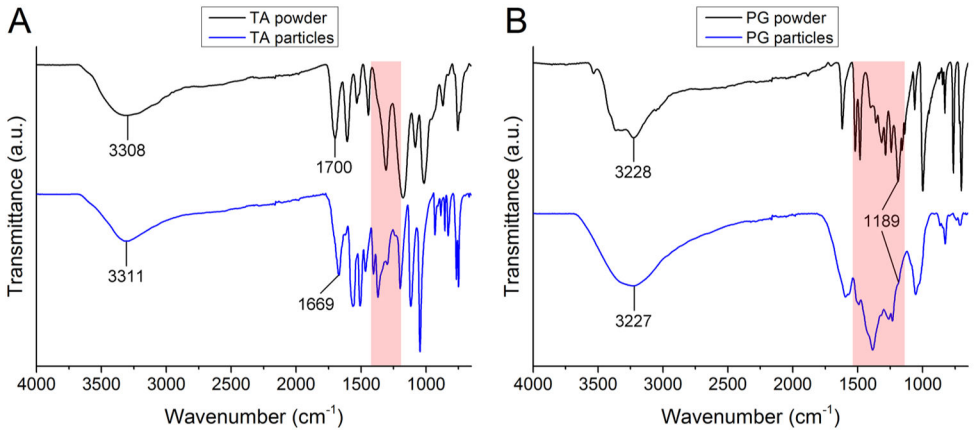

Figure 6.

Infrared spectra of precursor powders and polymerized polyphenol particles of (A) tannic acid (TA) and (B) pyrogallol (PG). Areas with most noticeable changes are highlighted.

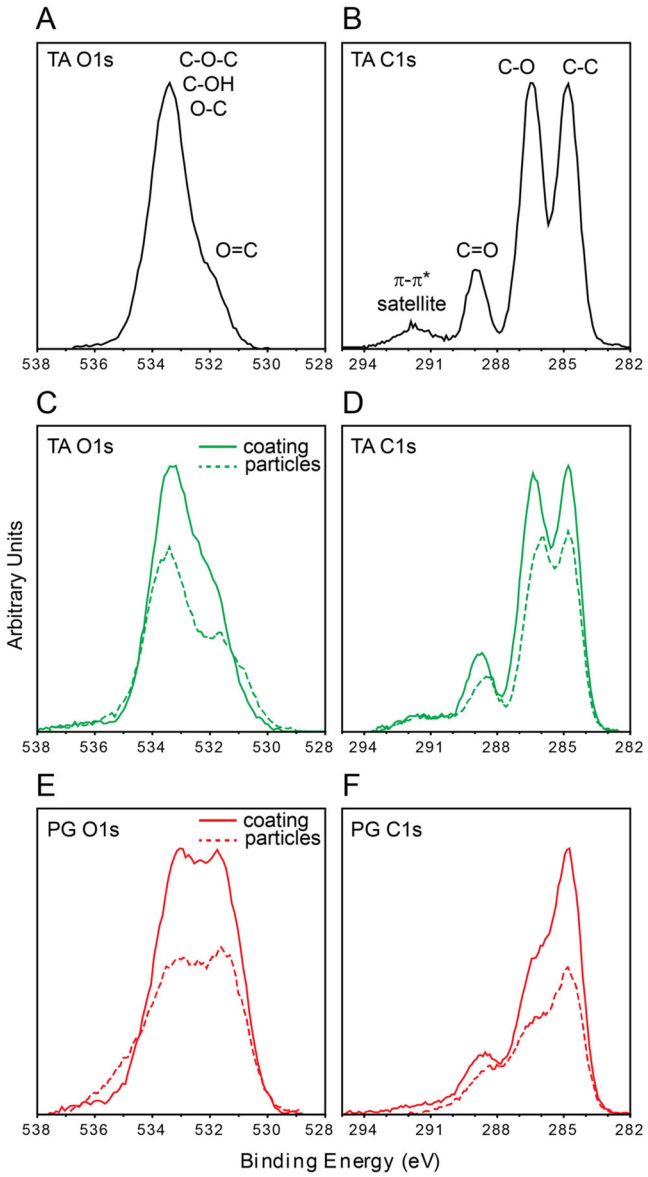

Figure 7.

XPS detail spectra. (A) O 1s of tannic acid (TA) precursor powder. (B) C 1s of TA precursor powder. (C) O 1s for TA coatings and polymerized TA particles. (D) C 1s for TA coatings and polymerized TA particles. (E) O 1s for pyrogallol (PG) coatings and polymerized PG particles. (F) C 1s for PG coatings and polymerized PG particles.

Table 1

XPS Element Distribution for Phenolic Precursor Powders, Coatings on Ti Discs, and Polymerized Particles[a]

	element distribution (at. %)						
	C	**O**	**Na**	**Mg**	**Cl**	**Si**	**C/O**
TA precursor	65.77	34.23	n.d.	n.d.	n.d.	n.d.	1.92
TA coating	60.64	34.51	3.69	n.d.	0.58	0.60	1.76
TA particles	59.83	35.10	4.29	n.d.	0.35	0.43	1.70
PG coating	67.14	29.89	n.d.	2.97	n.d.	n.d.	2.25
PG particles	65.64	31.48	n.d.	2.88	n.d.	n.d.	2.09

[a]The PG precursor powder could not be measured due to its high reactivity.

Theoretical C/O ratios for TA and PG are 1.65 and 2.00, respectively. A slight Si contamination was detected for TA coatings and particles. n.d. = not detected.